Geochemical Perspectives Letters

Aqueous concentration of CO_2 in carbon-saturated fluids as a highly sensitive oxybarometer

F. Miozzi[1]*, S. Tumiati[1]

OPEN ACCESS

doi: 10.7185/geochemlet.2040

Abstract

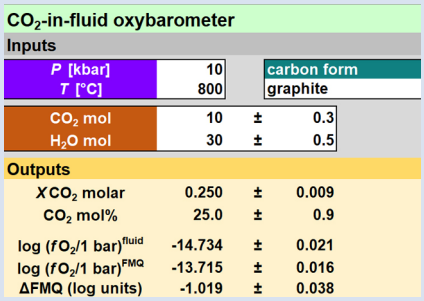

CO_2-in-fluid oxybarometer			
Inputs			
P [kbar]	10	carbon form	
T [°C]	800	graphite	
CO_2 mol	10	±	0.3
H_2O mol	30	±	0.5
Outputs			
XCO_2 molar	0.250	±	0.009
CO_2 mol%	25.0	±	0.9
log (fO_2/1 bar)^{fluid}	-14.734	±	0.021
log (fO_2/1 bar)^{FMQ}	-13.715	±	0.016
ΔFMQ (log units)	-1.019	±	0.038

The CO_2 content of aqueous fluids in equilibrium with carbon can be used to retrieve their oxygen fugacity if pressure and temperature are known. Applicable to both natural and experimental systems, we present a new oxybarometer based on the aqueous concentration of CO_2 in fluids saturated with either graphite or glass-like carbon, suitable to retrieve their oxygen fugacity. The method was experimentally tested by measuring by mass spectrometry the CO_2 content in aqueous fluids coexisting with glass-like carbon buffered externally with Ni-NiO, employing ordered and disordered forms of NiO characterised by small differences in free energy (<5 kJ/mol). Considering analytical uncertainties on CO_2 measurements, fO_2 values can be resolved with an accuracy of about 0.01 log units, which is one order of magnitude lower than uncertainties affecting conventional solid state redox sensors. The CO_2-in-fluid oxybarometer is the first available parameterisation of the fO_2 dependency on pressure, temperature and CO_2 content of aqueous fluids and can be used for fluids containing >1 mol. % CO_2 beneath the graphite-diamond transition.

Received 31 July 2020 | Accepted 5 November 2020 | Published 31 December 2020

Introduction

The definition and calibration of new and accurate oxybarometers aid in the investigation and interpretation of geological processes (*e.g.*, Arató and Audetat, 2017). As oxygen fugacity (fO_2) influences processes involving solids, aqueous fluids and melts, affecting phase equilibria and the behaviour of multivalent elements (*e.g.*, C, S, Fe), its precise determination is of primary importance.

All the chemical reactions dependent on fO_2 have the potential to serve as fO_2 sensors. Many mineral assemblages (*e.g.*, Ballhaus *et al.*, 1991), oxides and metal-oxide couples (*e.g.*, Tao *et al.*, 2017) and binary/ternary alloys (*e.g.*, Balta *et al.*, 2011) have been calibrated as solid oxybarometers and redox sensors, allowing the determination of fO_2 in both natural and experimental systems with an uncertainty of the order of 0.3 log units. Recently the aptness as oxybarometers of non-solid phases, for instance melts, where their CO_2 content depends on fO_2 (Stagno and Frost, 2010), has been shown. Using non-solid phases has the advantage of avoiding issues related to structure behaviour (phase transitions, melting processes *etc.*) at different pressure and temperatures.

Here we present the first calibration of an oxybarometer based on the CO_2 content of aqueous fluids. As carbon saturation constrains the fluid composition to the carbon-saturation surface, which is univariant in the COH system once the P-T conditions are fixed (*e.g.* Connolly, 1995; Tumiati and Malaspina, 2019), the independent definition of the fluid composition (*e.g.*, $XCO_2 = CO_{2,aq}/(H_2O + CO_{2,aq})_{molar}$) can be used to retrieve other intensive variables (*e.g.*, fO_2), and *vice versa*. In this study, we parameterised log (fO_2/1 bar)^{fluid} as a function of P, T and the fluid XCO_2. The ideal conditions for the application of the CO_2-in-fluid oxybarometer require an appreciable CO_2 content and carbon saturation. This means oxidised fluids, where XO (= O/H + O) > 1/3 (*e.g.*, Connolly and Cesare, 1993; Huizenga, 2001; Zhang and Duan, 2009) where there is saturation of ordered (graphite) or disordered (glass-like C) carbon. Glass-like carbon is considered an analogue of natural "disordered" carbon deriving from organic matter and has different thermodynamic properties in respect to graphite (*e.g.*, Tumiati *et al.*, 2020).

Parameterisation of the CO_2-in-fluid Oxybarometer

The fO_2 values of COH fluids in equilibrium with ideal graphite and glass-like C, a disordered but very homogenous X-ray amorphous graphitic carbon form often used in experimental petrology (*e.g.*, Spandler *et al.*, 2008), were fitted using a specific routine written in the Wolfram Mathematica® computation environment. The parametric equation Eq. 1, (P in kbar, T in °C and XCO_2 in mol. %) represents the best polynomial, evaluated statistically in more than 300 thousand other possible models (see Supplementary Information S-1). The fitted fO_2 values were calculated in the P-T-XCO_2 range 5–30 kbar, 600–1000 °C, 0.1–0.9 using the thermodynamic model from Zhang and Duan (2009), assessed by previous authors as the more robust fit to experimental data within those available (Tumiati *et al.*, 2020). The model was used in its original version for graphite-saturated fluid and with modified equilibrium constants (K_ps) for glass-like

1. Dipartimento di Scienze della Terra, Università degli Studi di Milano. Via Mangiagalli 34, 20133 Milano, Italy
* Corresponding author (email: miozzi.f@gmail.com)

C-saturated fluids (*cf.* Tumiati *et al.*, 2020) (see Supplementary Information S-2). Therefore, two sets of parameters (Table 1) were determined depending on the type of carbon considered (*i.e.* graphite or glass-like C).

$$\log(fO_2/1\ \text{bar})^{\text{fluid}} = a - (a_1/CO_2) + (a_2 \times CO_2) - (a_3 \times CO_2{}^2) + (a_4/P^2) - (a_5/P) + (a_6 \times P) + (a_7 \times CO_2 \times P^2) + (a_8 \times T) - (a_9 \times P \times T) - (a_{10} \times CO_2 \times P \times T) - (a_{11} \times P^2 \times T) - (a_{12} \times T^2) + (a_{13} \times CO_2 \times T^2) + (a_{14} \times P \times T^2) \quad \text{Eq. 1}$$

Table 1 Parameters of Eq. 1 provided for graphite and glass-like C. Numbers in parentheses indicate the standard error.

	Graphite	Glass-like C
a	−48.85(7)	−49.03(8)
a_1	−4.3(1)	−4.3(1)
a_2	0.0115(4)	0.0114(4)
a_3	$-4(3)\cdot10^{-5}$	$-4(3)\cdot10^{-5}$
a_4	19(2)	17(2)
a_5	−9.4(6)	−8.9(6)
a_6	0.287(2)	0.291(3)
a_7	$1(3)\cdot10^{-6}$	$1(3)\cdot10^{-6}$
a_8	0.0690(1)	0.0690(1)
a_9	$-4(1)\cdot10^{-4}$	$-4(1)\cdot10^{-4}$
a_{10}	$-8(2)\cdot10^{-8}$	$-1(2)\cdot10^{-7}$
a_{11}	$-2(1)\cdot10^{-7}$	$-2(1)\cdot10^{-7}$
a_{12}	$-3(1)\cdot10^{-5}$	$-3(1)\cdot10^{-5}$
a_{13}	$2(3)\cdot10^{-9}$	$2(3)\cdot10^{-9}$
a_{14}	$2(5)\cdot10^{-7}$	$2(6)\cdot10^{-7}$
Average residuals (log units)	0.005	0.005

The average residuals, 0.005 log units (Table 1), represent the uncertainty of the model (see also Fig. S-1). This value does not take into account the uncertainties associated with the measurement of CO_2 in aqueous fluids, which is of the order of 1 mol. % for quadrupole mass spectrometry analyses (Tiraboschi *et al.*, 2016 and Tumiati *et al.*, 2020). Accordingly, we performed a series of experiments to evaluate realistic uncertainties associated with the CO_2-in-fluid oxybarometer and assess its sensitivity to resolve small variations of oxygen fugacity.

Testing the CO_2-in-fluid Oxybarometer: Carbon-saturated Fluids Buffered with Ni-NiO

The nickel-nickel oxide (NNO) oxygen buffer, whose position in the P-T-fO_2 field depends on the thermodynamic properties of the Ni and NiO, was used to control externally the oxygen fugacity (and therefore the CO_2 content) of a glass-like C saturated aqueous fluid. Different NiO reagents have slightly different thermodynamic properties (*e.g.*, O'Neill and Pownceby, 1993). We built up the buffering assemblages employing different NiO precursors to test the sensitivity of the oxybarometer and investigate their thermodynamic properties. Reagent grade Ni metal powder was mixed with: (i) two commercial nickel oxide nanopowders, green and black, with an average crystallite size of 100 and 10 nm respectively; (ii) sintered nickel oxide, produced by heating green nanopowder for three days at 1300 °C and (iii) nickel hydroxide ($Ni(OH)_2$), which decomposes to NiO at T > 230 °C (details in Supplementary Information S-3, Fig. S-2). As a source of carbon, glass-like C, a NIST standard material (Cappelletti *et al.*, 2018) was preferred to graphite in order to avoid impurities often present in natural samples and to have a material with well characterised thermodynamic properties (*cf.* Tumiati *et al.*, 2020).

Experiments were performed using the double capsule (*e.g.*, Eugster and Skippen, 1967) and the triple capsule (Matjuschkin *et al.*, 2015) techniques (Fig. S-4) to avoid the direct contact of the fluids with the NNO buffer. Fluids were equilibrated at 10 kbar and 800 °C for 24 hours in an end load piston cylinder. After the experiments, quenched capsules were pierced in a gas tight vessel and the gases conveyed to a quadrupole mass spectrometer (QMS) for the analysis of volatiles (Tiraboschi *et al.*, 2016).

On the basis of the measured CO_2 content, we retrieved the log fO_2 of the fluids using: (i) the thermodynamic calculations suggested by Tumiati *et al.*, (2017) and Tumiati *et al.*, (2020), and (ii) the CO_2-in-fluid oxybarometer (Table 2). The susceptibility of XCO_2 to fO_2 variations gives the methodology enough sensitivity to see variations of 0.001 log units. The uncertainties on fO_2 value, propagated from the analytical error on the XCO_2, are of the order of 0.01 log units. The results obtained by thermodynamic calculations are well reproduced by the CO_2-in-fluid oxybarometer, with the constant discrepancy of 0.02 being the result of the different equilibrium constants (K_ps) used. Those derived from experiments (Tumiati *et al.*, 2020) for the thermodynamic calculations (Table 2) and those obtained by modelling the thermodynamic properties (*cf.* "Parameterisation of the CO_2-in-fluid oxybarometer" above) for the CO_2-in-fluid oxybarometer (Table 2).

With the fluid's log fO_2, fH_2 can be retrieved and used to obtain the log fO_2 of the buffering assemblage (see Supplementary Information S-4 for the procedure), thus allowing comparison with the NNO reference calculated with Perple_X (Connolly, 2005) and the hp04ver.dat thermodynamic database updated with the most recent re-assessment for both Ni and NiO of ΔG_f^0 and S^0 (Gamsjäger *et al.*, 2005) and equation of state parameters K_0 and K_0' (Campbell *et al.*, 2009) (Table 2).

Within the different buffering assemblages, those made with black nickel oxide and sintered nickel oxide reproduce the reference fO_2 better. The discrepancy in the oxygen fugacity imposed by the sintered, in comparison to standard green NiO, confirms the need to sinter the material to increase its reactivity, as previously reported in literature (*e.g.*, Mattioli and Wood, 1988; O'Neill and Pownceby, 1993). For black nickel oxide, the high temperature of the experiments coupled with the long duration likely induced the sintering of this disordered material (*cf.* TEM images, Fig. 1a) during the experimental run, hence the imposed fO_2 closely reproduces the NNO reference. As such, its usage for experiments at low T or of short duration is discouraged without previous sintering. Sintering during the experimental run is not easily achieved for the NiO green nanopowder, due to its relatively ordered (and therefore stable) state, with larger sizes and well shaped crystals (*cf.* TEM images, Fig. 1b).

Finally, the retrieved fO_2 of the buffering assemblages were used to determine the Gibbs free energy of formation (ΔG_f^0) of the different NiO reagents and subsequently model the evolution in temperature of their log fO_2 (Fig. 1c).

Using the dependency between the two parameters, we iteratively changed the ΔG_f^0 for NiO in the updated hp04ver.dat thermodynamic database of Perple_X, to match the fO_2 derived from the measured fluid compositions. Compared to the NNO reference, the minimum variation in ΔG_f^0 detected is 0.7 KJ mol^{-1} for a 0.07 log fO_2 variation. The fO_2 imposed by the different

Table 2 Run table including CO_2 measured in the experimental aqueous fluids. fO_2 resulting from the thermodynamic modelling of glass-like C-saturated fluids buffered at 10 kbar and 800 °C and derived free energies of formation of different nickel oxide precursors are provided. Numbers in parentheses indicate the standard error.

Exp. no.	Buffer	XCO_2 COH fluid (meas.)	log fO_2 COH fluid (inner capsule)[a]	log fO_2 COH fluid (inner capsule)[b]	fH_2 COH inner = outer[a]	log fO_2 buffer (outer capsule)[c]	ΔG_f^0 NiO (KJ mol^{-1})	ΔG NiO (reference-experimental) (KJ mol^{-1})
COH54	NiO (from green nanopowder) + Ni	0.751(5)	−14.337(3)	−14.317(1)	103(3)	−13.94(2)	−215.7(2)	4.2
COH59[d]	NiO (from green nanopowder) + Ni	0.786(6)	−14.316(3)	−14.295(1)	84(3)	−13.77(3)	−213.7(3)	2.4
COH37	NiO (from black nanopowder) + Ni	0.815(4)	−14.300(2)	−14.279(1)	70(2)	−13.61(3)	−212.2(3)	0.7
COH42	Ni + NiO (from $Ni(OH)_2$)	0.866(2)	−14.274(1)	−14.252(1)	48(1)	−13.27(2)	−208.7(2)	−2.7
COH45	Ni + NiO (from $Ni(OH)_2$)	0.857(3)	−14.278(2)	−14.257(1)	51(2)	−13.33(3)	−209.6(2)	−2.1
COH57	NiO (from sintered green nanopowder) + Ni	0.850(6)	−14.282(3)	−14.260(1)	58(3)	−13.39(4)	−210.1(4)	−1.5
Reference	Ni + NiO	0.827	−14.294	–	64	−13.54	−211.7	–

[a] EoS by Zhang and Duan (2009) modified to include the dynamic γH_2 taken from Connolly and Cesare (1993), changing as a function of P, T and XO ($\gamma H_2 = A \bullet (XO)^3 + B \bullet (XO)^2 + C \bullet XO + D$; where $A = 43.919$, $B = 114.55$, $C = -105.75$, $D = 41.215$ at 10 kbar and 800 °C; $A = -11208$; $B = 26723$, $C = -21949$, $D = 6979.2$ at 3 GPa and 800 °C) (Tumiati *et al.*, 2017), and the equilibrium constants (K_ps) for glass-like C from Tumiati *et al.*, (2020).
[b] retrieved with the CO_2-in-fluid oxybarometer
[c] retrieved using the routine "fluids" of the Perple_X package (H-O HSMRK/MRK hybrid EoS).
ΔG_f^0 Gibbs free energy of formation from the elements in their standard state (298 K; 1 bar). Determined by changing the thermodynamic database hp04ver.dat in the Perple_X computer package (http://www.perplex.ethz.ch; Connolly, 2005) to match the oxygen fugacity obtained using different nickel oxide precursors in the buffer.
ΔG NiO = ΔG_f^0 NNO reference – ΔG_f^0 NNO experimental.
[d] triple capsule design. Two smaller capsules, respectively containing the carbon-saturated fluid and the buffering assemblage, are vertically positioned on top of each other and inside a bigger capsule, embedded in Al_2O_3 (Matjuschkin *et al.*, 2015).

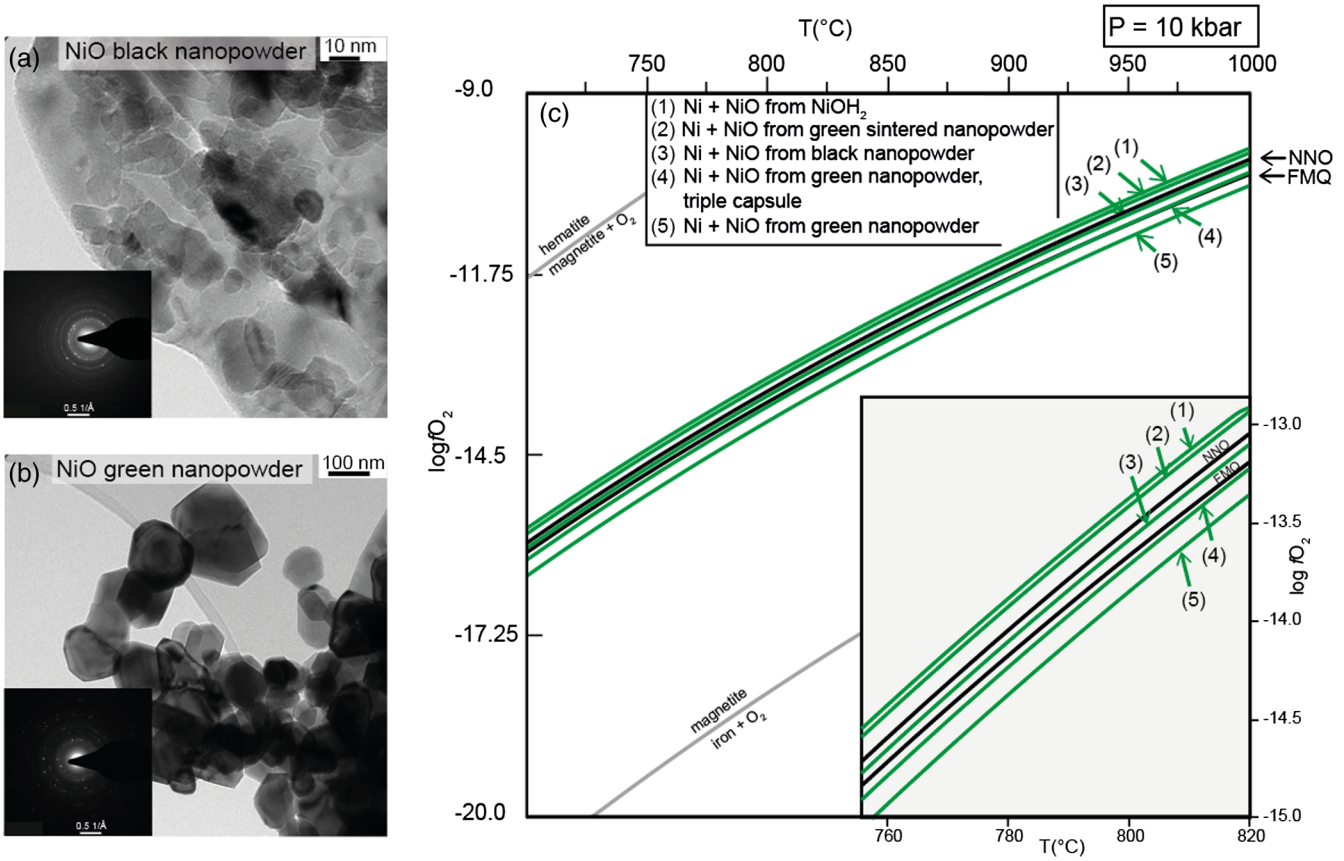

Figure 1 **(a)** and **(b)** Transmission electron microscopy images and diffraction rings (insets) of the two commercial NiO nanopowders used as reagents in the buffering assemblages. **(c)** Isobaric evolution of the NNO buffer oxygen fugacity for buffering assemblages with different NiO reagents (green lines). Black lines represent the evolution predicted by thermodynamic models of the NNO and FMQ buffers. The line representing FMQ (fayalite + O_2 = magnetite + quartz), iron + O_2 = magnetite and magnetite + O_2 = hematite buffers are provided for reference.

precursors have a consistent evolution in the investigated T range. While the assemblages with black NiO, sintered NiO and $Ni(OH)_2$ plot closer to the NNO reference, green NiO plots even below the FMQ equilibrium. The different capsule assemblage (*i.e.* triple instead of double) slightly increases the fO_2 but not enough to reach the reference. Accordingly NiO sintering before the experiments is needed in order to impose an fO_2 close to the thermodynamic reference.

Applications

The CO_2-in-fluid oxybarometer has been calibrated for CO_2-dominated aqueous fluids saturated in carbon, either ordered (graphite) or disordered (glass-like C) and can be used at P-T-pH conditions where the carbon-bearing dissolved species mostly exist in their molecular state (*i.e.* $CO_{2,aq}$) and not as charged anionic or cationic species (Sverjensky *et al.*, 2014; Tumiati *et al.*, 2020).

The model is easily accessible in the CO_2-in-fluid Excel spreadsheet available for download in the Supplementary Information. The calculation requires as input data P, T, XCO_2 and the type of carbon considered (*i.e.* graphite or glass-like C). The calculator provides the COH fluid's fO_2 and its uncertainties both expressed as absolute value (log unit) and in relation to the FMQ reference (*i.e.* $\Delta FMQ = \log fO_2^{FMQ} - \log fO_2$) as well as the fO_2 for the FMQ reference itself. The latter is calculated using an improved parameterisation, established in the present study in order for the uncertainties to be consistent with those determined for the oxybarometer (see Supplementary Information S-5). In particular, the average residuals of the present FMQ fit are 0.01629 and the maximum 0.09674 while the commonly used equation, established by O'Neill (1987), has average and maximum residuals of 0.06347 and 0.32023 respectively.

The extensive use of fluids in experimental petrology guarantees a wide range of applications in this field. The CO_2-in-fluid oxybarometers give the opportunity to retrieve the oxygen fugacity of the studied system in experiments focused on fluids or fluid-rock interactions (*e.g.* Stagno and Frost, 2010) and those involving a glass-like C melt-trap or graphite linings to isolate the capsule from the experimental charge (*e.g.*, Spandler *et al.*, 2008; Tiraboschi *et al.*, 2018). Its use is also extended to double capsule buffered experiments where it represents a helpful tool to assess the attainment of equilibrium on the basis of the expected fO_2 conditions, thus excluding any influence of the experimental assembly. Using the XCO_2 to determine the fO_2 in experiments involving fluids represents a reliable and more accurate alternative to solid state sensors provided attainment of the needed conditions. It would avoid potential issues related to the possible interaction of the solid sensor with the starting materials, which would modify the initial petrological system, and to the possible disequilibrium composition of solid state sensors, *e.g.*, alloys, in low T experiments.

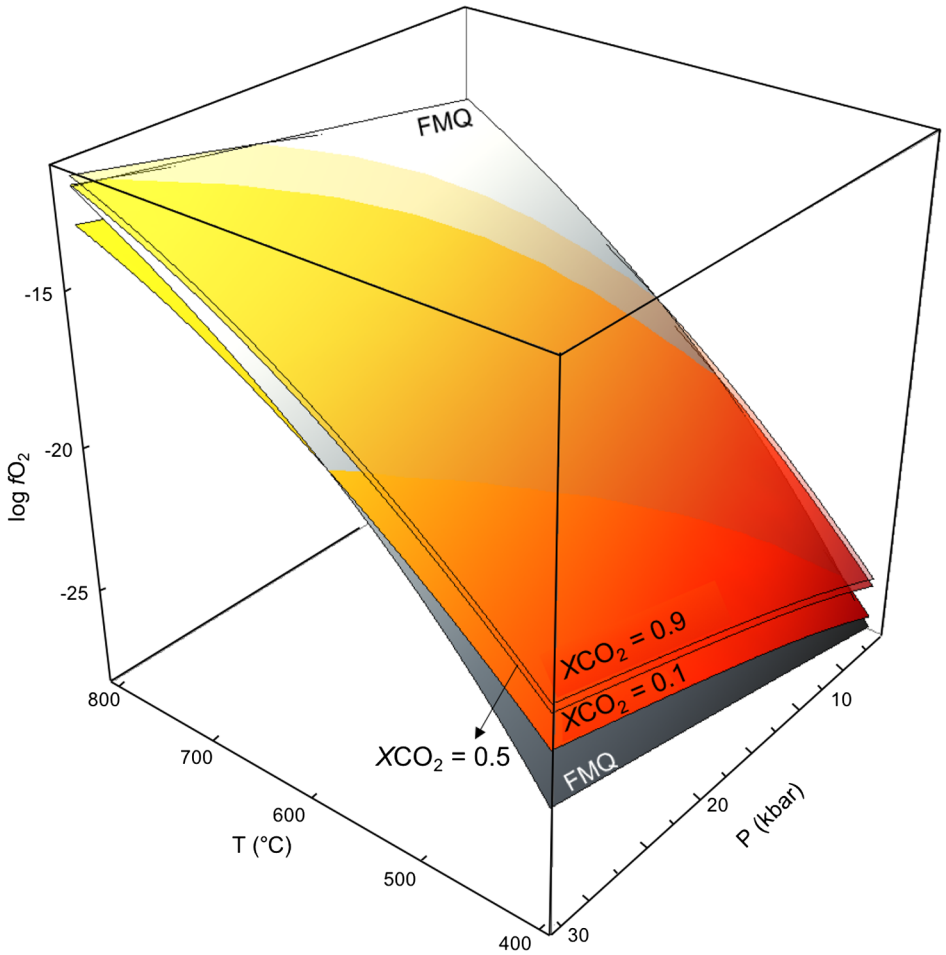

Figure 2 Graphite saturated COH fluid in the P-T-log fO_2 space. Coloured surfaces represent isopleths of low (0.1), intermediate (0.5) and high (0.9) CO_2 content in the COH fluid expressed as XCO_2 ($XCO_2 = CO_2/(CO_2 + H_2O)$). The grey shaded FMQ surface represents the univariant equilibrium of the reaction: $2\ Fe_3O_4 + 3\ SiO_2 = 3\ Fe_2SiO_4 + O_2$.

The CO_2-in-fluid oxybarometer could be a useful tool also in natural systems, provided that some important requirements are met. The most important is the attainment of equilibrium between carbon and COH fluid. This is not a trivial issue. For instance, previous studies showed that graphite is poorly reactive below 500–600 °C (Ziegenbein and Johannes, 1980; Luque *et al.*, 1998). At these low temperatures, thermodynamic equilibrium is hampered by slow kinetics, thus implying that results coming from thermodynamic modelling of COH fluids in equilibrium with carbon, independently from the chosen model, should be handled with care. Another variable that obviously could affect the approach to equilibrium is time. Short lived processes or an opening of the system could result in fluids that are not representative of the equilibrium state. Finally, the complexity of the systems should also be taken into account as complex systems might have a different CO_2 content with respect to the pure COH (*e.g.*, SiO_2-bearing, Tumiati *et al.*, 2017).

Acknowledgements

Authors are indebted to A. Risplendente for the assistance at scanning electron microscope and electron microprobe, to N. Rotiroti for the assistance with the transmission electron microscope and to C. Tiraboschi for preparing some of the experiments. FM and ST acknowledge support of the Italian program MIUR PRIN 2017ZE49E7_002.

Editor: Eric H. Oelkers

Additional Information

Supplementary Information accompanies this letter at https://www.geochemicalperspectivesletters.org/article2040.

Cite this letter as: Miozzi, F., Tumiati, S. (2020) Aqueous concentration of CO_2 in carbon-saturated fluids as a highly sensitive oxybarometer. *Geochem. Persp. Let.* 16, 30–34.

References

Arató, R., Audétat, A. (2017) FeTiMM–A new oxybarometer for mafic to felsic magmas. *Geochemical Perspectives Letters* 5, 19–23.

Balta, J.B., Beckett, J.R., Asimow, P.D. (2011) Thermodynamic properties of alloys of gold-74/palladium-26 with variable amounts of iron and the use of Au-Pd-Fe alloys as containers for experimental petrology. *American Mineralogist* 96, 1467–1474.

Ballhaus, C., Berry, R.F., Green, D.H. (1991) High pressure experimental calibration of the olivine-orthopyroxene-spinel oxygen geobarometer: implications for the oxidation state of the upper mantle. *Contributions to Mineralogy and Petrology* 107, 27–40.

Campbell, A.J., Danielson, L., Righter, K., Seagle, C.T., Wang, Y., Prakapenka, V.B. (2009) High pressure effects on the iron–iron oxide and nickel–nickel oxide oxygen fugacity buffers. *Earth and Planetary Science Letters* 286, 556–564.

Cappelletti, R.L., Udovic, T.J., Li, H., Paul, R.L. (2018) Glassy carbon, NIST Standard Reference Material (SRM 3600): hydrogen content, neutron vibrational density of states and heat capacity. *Journal of Applied Crystallography* 51, 1323–1328.

Connolly, J.A.D. (1995) Phase diagram methods for graphitic rocks and application to the system C–O–H–FeO–TiO_2–SiO_2. *Contributions to Mineralogy and Petrology* 119, 94–116.

Connolly, J.A. (2005) Computation of phase equilibria by linear programming: a tool for geodynamic modeling and its application to subduction zone decarbonation. *Earth and Planetary Science Letters* 236, 524–541.

Connolly, J.A.D., Cesare, B. (1993) C-O-H-S Fluid Composition and Oxygen Fugacity in Graphitic Metapelites. *Journal of Metamorphic Geology* 11, 379–388.

Eugster, H.P., Skippen, G.B. (1967) Igneous and metamorphic reactions involving gas equilibria. *Researches in Geochemistry* 2, 492–520.

Gamsjäger, H., Bugajski, J., Preis, W. (2005) *Chemical thermodynamics of nickel*. Elsevier, Amsterdam.

Luque, F.J., Pasteris, J.D., Wopenka, B., Rodas, M., Fernández Barrenechea, J.M. (1998) Natural fluid-deposited graphite: mineralogical characteristics and mechanisms of formation. *American Journal of Science* 298, 471–498.

Huizenga, J.M. (2001). Thermodynamic modelling of C–O–H fluids. *Lithos* 55, 101–114.

Matjuschkin, V., Brooker, R.A., Tattitch, B., Blundy, J.D., Stamper, C.C. (2015) Control and monitoring of oxygen fugacity in piston cylinder experiments. *Contributions to Mineralogy and Petrology* 169, 9.

Mattioli, G.S., Wood, B.J. (1988) Magnetite activities across the $MgAl_2O_4$-Fe_3O_4 spinel join, with application to thermobarometric estimates of upper mantle oxygen fugacity. *Contributions to Mineralogy and Petrology* 98, 148–162.

O'Neill, H.S. (1987). Quartz-fayalite-iron and quartz-fayalite-magnetite equilibria and the free energy of formation of fayalite (Fe_2SiO_4) and magnetite (Fe_3O_4). *American Mineralogist,* 72(1-2), 67–75.

O'Neill, H.S.C., Pownceby, M.I. (1993) Thermodynamic data from redox reactions at high temperatures. I. An experimental and theoretical assessment of the electrochemical method using stabilized zirconia electrolytes, with revised values for the Fe-"FeO", Co-CoO, Ni-NiO and Cu-Cu_2O oxygen buffers, and new data for the W-WO_2 buffer. *Contributions to Mineralogy and Petrology* 114, 296–314.

Spandler, C., Yaxley, G., Green, D.H., Rosenthal, A. (2008) Phase relations and melting of anhydrous K-bearing eclogite from 1200 to 1600 C and 3 to 5 GPa. *Journal of Petrology* 49, 771–795.

Stagno, V., Frost, D.J. (2010). Carbon speciation in the asthenosphere: Experimental measurements of the redox conditions at which carbonate-bearing melts coexist with graphite or diamond in peridotite assemblages. *Earth and Planetary Science Letters* 300, 72–84.

Sverjensky, D.A., Stagno, V., Huang, F. (2014) Important role for organic carbon in subduction-zone fluids in the deep carbon cycle. *Nature Geoscience* 7, 909–913.

Tao, R., Zhang, L., Stagno, V., Chu, X., Liu, X. (2017) High-Pressure experimental verification of rutile-ilmenite oxybarometer: Implications for the redox state of the subduction zone. *Science China Earth Sciences* 60, 1817–1825.

Tiraboschi, C., Tumiati, S., Recchia, S., Miozzi, F., Poli, S. (2016) Quantitative analysis of COH fluids synthesized at HP–HT conditions: an optimized methodology to measure volatiles in experimental capsules. *Geofluids* 16, 841–855.

Tiraboschi, C., Tumiati, S., Sverjensky, D., Pettke, T., Ulmer, P., Poli, S. (2018) Experimental determination of magnesia and silica solubilities in graphite-saturated and redox-buffered high-pressure COH fluids in equilibrium with forsterite+enstatite and magnesite+enstatite. *Contributions to Mineralogy and Petrology* 173, 2.

Tumiati, S., Malaspina, N. (2019) Redox processes and the role of carbon-bearing volatiles from the slab–mantle interface to the mantle wedge. *Journal of the Geological Society* 176, 388–397.

Tumiati, S., Tiraboschi, C., Sverjensky, D.A., Pettke, T., Recchia, S., Ulmer, P., Miozzi, F., Poli, S. (2017) Silicate dissolution boosts the CO 2 concentrations in subduction fluids. *Nature Communications* 8, 1–11.

Tumiati, S., Tiraboschi, C., Miozzi, F., Vitale-Brovarone, A., Manning, C.E., Sverjensky, D.A., Milani, S., Poli, S. (2020) Dissolution susceptibility of glass-like carbon versus crystalline graphite in high-pressure aqueous fluids and implications for the behavior of organic matter in subduction zones. *Geochimica et Cosmochimica Acta* 273, 383–402.

Ziegenbein, D., Johannes, W. (1980) Graphite in CHO fluids: An unsuitable compound to buffer fluid composition at temperatures up to 700°C. *Neues Jahrbuch fur Mineralogie-Monatshefte 7,* 289–305.

Zhang, C., Duan, Z. (2009) A model for C–O–H fluid in the Earth's mantle. *Geochimica et Cosmochimica Acta* 73, 2089–2102.

Geochemical Perspectives Letters

Aqueous concentration of CO_2 in carbon-saturated fluids as a highly sensitive oxybarometer

F. Miozzi, S. Tumiati

Supplementary Information

The Supplementary Information includes:

- CO_2-in-fluid Oxybarometer (Excel Spreadsheet)
- S-1 Details on the Evaluation of the Best Fit Model
- S-2 Modelling of Glass-like C Saturated COH Fluids for the Calibration of the Oxybarometer
- S-3 NiO Reagents and Starting Materials
- S-4 Thermodynamic Modelling in Double and Triple Capsule Experiments
- S-5 Parameterisation of the fO_2 Dependency from P and T for the Fayalite-Quartz-Magnetite (FMQ) Equilibrium
- Figures S-1 to S-4
- Supplementary Information References

CO_2-in-fluid Oxybarometer (Excel Spreadsheet)

The CO_2-in-fluid Excel spreadsheet is available for download from the online version of the article at http://www.geochemicalperspectivesletters.org/article2040.

S-1 Details on the Evaluation of the Best Fit Model

The program, in order to determine the best fitting model, first generate a list of all the possible equations, defined by the provided variables, and fitting the given data. Within all the possible equations, the best fit solution is the one with the higher quality according to four different statistical criteria. R^2 and the Adjusted R^2, defining how close the model is to the observed data. In respect to R^2, the adjusted R^2 is also modified to account for the number of parameters considered in the model. AIC and BIC, respectively the Aikake information criteria and the Bayesian information criteria that are based on the likelihood function and serve to assess the quality of the model. Also these two criteria take in account the number of parameters, as both have a penalisation term if their number is high. While R^2 and the Adjusted R^2 have a value comprised between 0 and 1, where at 1 the model coincide with

the observed data, the lower is the value for AIC and BIC, higher is the quality of the fit. In the present study the chosen model is the one that minimise the value of the AIC.

S-2 Modelling of Glass-like C Saturated COH Fluids for the Oxybarometer's Calibration

Modelling the composition of a COH fluid saturated with glass-like C instead of graphite requires the use of different equilibrium constants (K_ps) for the reactions involving carbon (see equations (6)-(9) in Tumiati *et al*,. 2020).

The variation of K_ps depends on the difference in the Gibbs free energy (*i.e*. ΔG) between graphite and glass-like C. Once the ΔGs for both type of carbon are calculated, it is possible to use the standard K_ps and those determined by Tumiati *et al.* (2020) for glass-like C (at 10 Kbar and 800 °C), to establish the constant relating the difference in ΔGs and the difference in K_ps. Such constant is the same at all pressure and temperatures, hence, knowing the ΔGs it is possible to use these two parameters to calculate the K_ps at all P and T conditions. The Gibbs free energy of formation of both graphite and glass-like C were calculated using the routine "Frendly" in the Perple_X package (Connolly 2005; http://www.perplex.ethz.ch/), with the hp04ver.dat thermodynamic database modified to include glass-like carbon with the preferred model as in Tumiati *et al.*, (2020).

As carbon saturated COH fluids at fixed P, T condition are thermodynamically univariant, the oxygen fugacity is constrained once the composition is known, hence it is possible to determine the fO_2 from XCO_2 and vice-versa. Accordingly, we used the solver tool on the Gfluid Excel spreadsheet (Zhang and Duan 2009) and providing the XCO_2 value retrieved from the experiment, the program iteratively changed the oxygen fugacity until the calculated fluid composition matched the given one. The standard version of the spreadsheet was used for graphite saturated COH fluids. Conversely, for glass-like C saturated fluids, the equilibrium constants of the reactions involving carbon were replaced with those calculated following Tumiati *et al.* (2020).

S-3 NiO Reagents and Starting Materials for the Experiments

The two commercial nickel oxides were respectively nickel oxide black nanopowder (Sigma-Aldrich Product 72257) and nickel oxide green nanopowder (Sigma-Aldrich. Product 399523-100G). Sintered nickel oxide, was obtained sintering in air a batch of NiO green nanopowder at 1300°C for 72 h. $Ni(OH)_2$ was produced drying at 75°C the product of the basification of a $NiCl_2$ solution with $Na(OH)_2$.
Oxalic acid dihydrate (OAD) which decomposes at T> 200 °C to CO_2, H_2O and H_2, was used as a fluid source and glass-like C as the carbon reservoir. Their addition to the list of NIST's standards list and thorough thermodynamic characterization from Tumiati and co-authors (2020).

S-4 Thermodynamic Modelling in Double and Triple Capsule Experiments

In double and triple capsule experiments the buffer reaction with water controls the hydrogen fugacity ($f H_2$) in the outer capsule (eq. 1 in Tumiati *et al.*, 2020). Thanks to the permeability of the inner capsule to H_2, the $f H_2$ equilibrium in the inner capsule is reached with $f H_2$-dependent reactions (eq. 4 and 5 in Tumiati *et al.*, 2020) taking place in the GCOH fluid.

Accordingly, using fH_2 as a constrain and the proper equations of state (i.e. modelling a CO_2-H_2O fluid in the inner capsule and H_2O fluid in the outer capsule), it is possible to retrieve the log fO_2 of the fluid in the inner capsule from the buffer's fO_2 and vice-versa.

The GFluid Excel spreadsheet and the Zhang and Duan (2009) COH fluid EoS were used for the COH fluids, using the solver obtains fH_2 from the XCO_2 of the experiments and to determine XCO_2 form the fH_2 of the NNO reference. For the experiments, once the fH_2 is known, the fO_2 of the buffering assemblages is obtained by tabulating all the possible values, with the X(O) H-O HSMRK/MRK hybrid-EoS from the "fluids" routine in Perple_X (Connolly 2005; http://www.perplex.ethz.ch/) and finding the one that corresponds to the obtained fH_2.
For the NNO reference instead, the fO_2 of the buffering assemblage at the desired P-T conditions was calculated with the "vertex" routine in Perple_X and used to determine the corresponding fH_2 from the values tabulated with the X(O) H-O HSMRK/MRK hybrid-EoS from the "fluids" routine.

S-5 Parameterisation of the fO_2 Dependency from P and T for the Fayalite-Magnetite-Quartz (FMQ) Oxygen Buffer

Commonly used references for the FMQ buffer (*e.g.*, Ohmoto and Kerrick 1977, O'Neill 1987, Ballhaus *et al.*, 1991) have an average uncertainty on the fO_2 calculation of 0.06 log unit. In the present study the uncertainty on the parameterisation of the fO_2 for COH fluids is one order of magnitude lower (*i.e.* 0.005 log units). Accordingly, in order to define the fO_2 also in term of ΔFMQ, an estimate of fO_2 for FMQ with a compatible uncertainty is needed.

We parameterised the fO_2 dependency of the FMQ buffer from P and T using the same fitting routine as for the parameterisation of the CO_2-in-fluid oxybarometer. The data used for the fit were calculated with the "vertex" routine of the Perple_X package (Connolly 2005). The resulting parametrisation with P in Kbar, T in °C and XCO_2 in mol % is:

$$\text{Log } fO_2^{FMQ} = -320.83 + (0.156252/P^2) - (0.20758/P) + (0.111218 \cdot P) - (0.00015537 \cdot P^2) - (82144.7/T^2) + (3876.2/T) + ((21.7 \cdot P)/T) - (0.057 \cdot T) - (0.000051 \cdot P \cdot T) + 50.66 \cdot \log(T) \quad \text{Eq. S-1}$$

The associated uncertainty is in the order of 0.01 log units.

Supplementary Figures

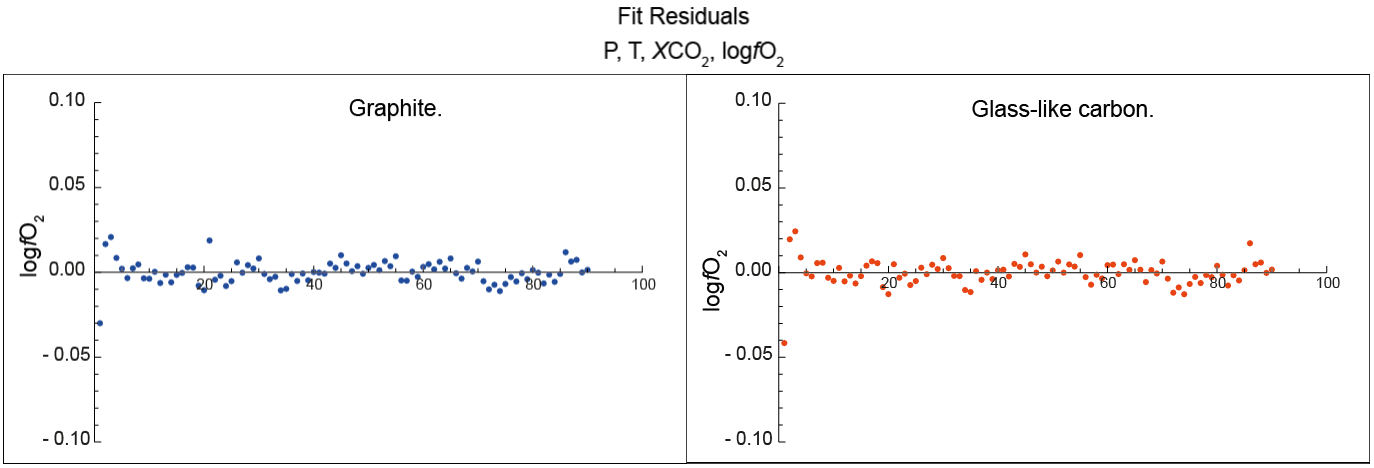

Figure S-1 Residuals from the fit of COH fluids' data with the chosen polynomial equation. Each point represents the difference between the fO_2 value from the experiments and the fO_2 calculated with the model. The results obtained for fluids in equilibrium with graphite (on the left) and glass-like C (on the right) are shown.

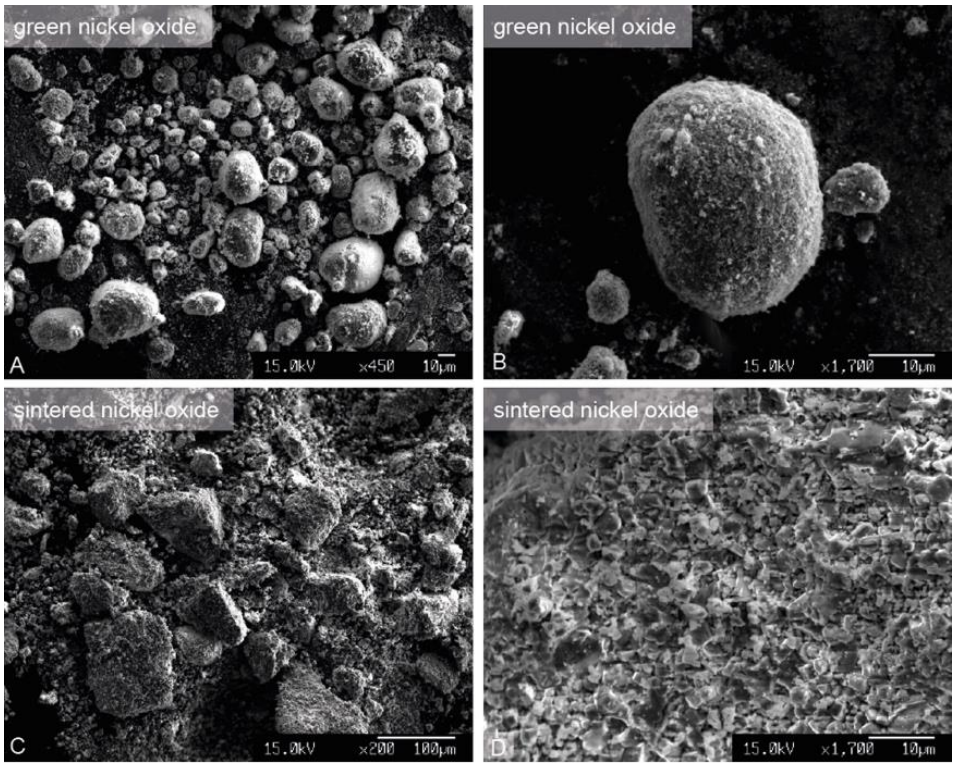

Figure S-2 Scanning electron microscope images of commercial nickel oxide green nanopowder before and after sintering, taken at 15 KeV. The two different magnifications chosen for each compound offer a better visualisation of the differences in the granulometry and grain distribution.

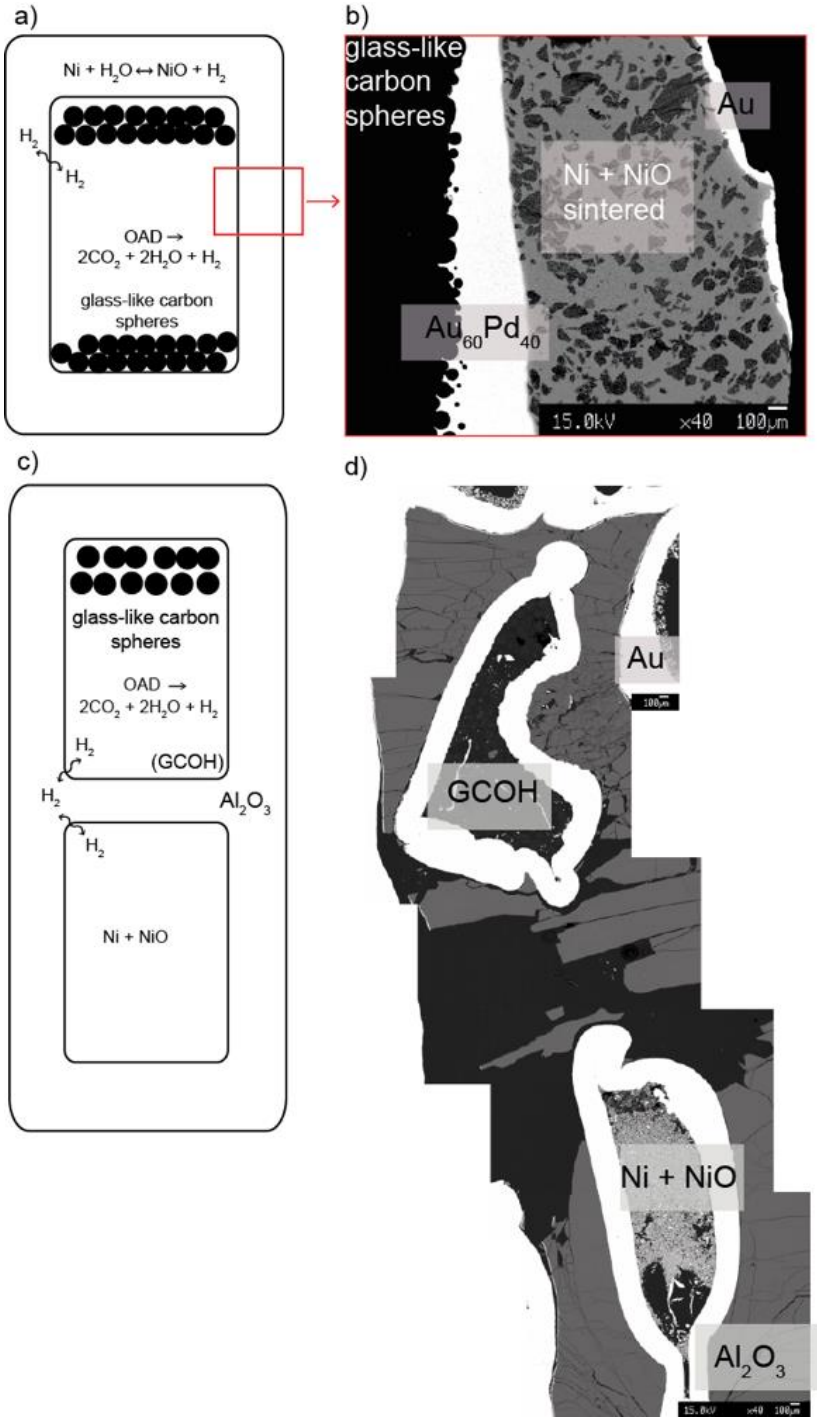

Figure S-3 Left side: schemes of the double **(a)** and triple **(c)** capsules used for the experiments. Inner capsule are made in $Au_{60}Pd_{40}$ (OD = 2.3 mm) and the outer in Au (OD = 5 mm).
The inner capsule, permeable to H_2 contains oxalic acid dihydrate which decomposes at T> 200 °C to CO_2, H_2O and H_2, and glass-like carbon. In the double capsule it is embedded in the buffering nickel + nickel oxide (+H_2O) assemblage and placed into the outer capsule. In the triple a second inner capsule is filled with the buffering assemblage and both are positioned in the external capsule, embedded in Al_2O_3.
Right side: backscattered electron images of a double **(b)** and triple capsule **(d)** representative portion.

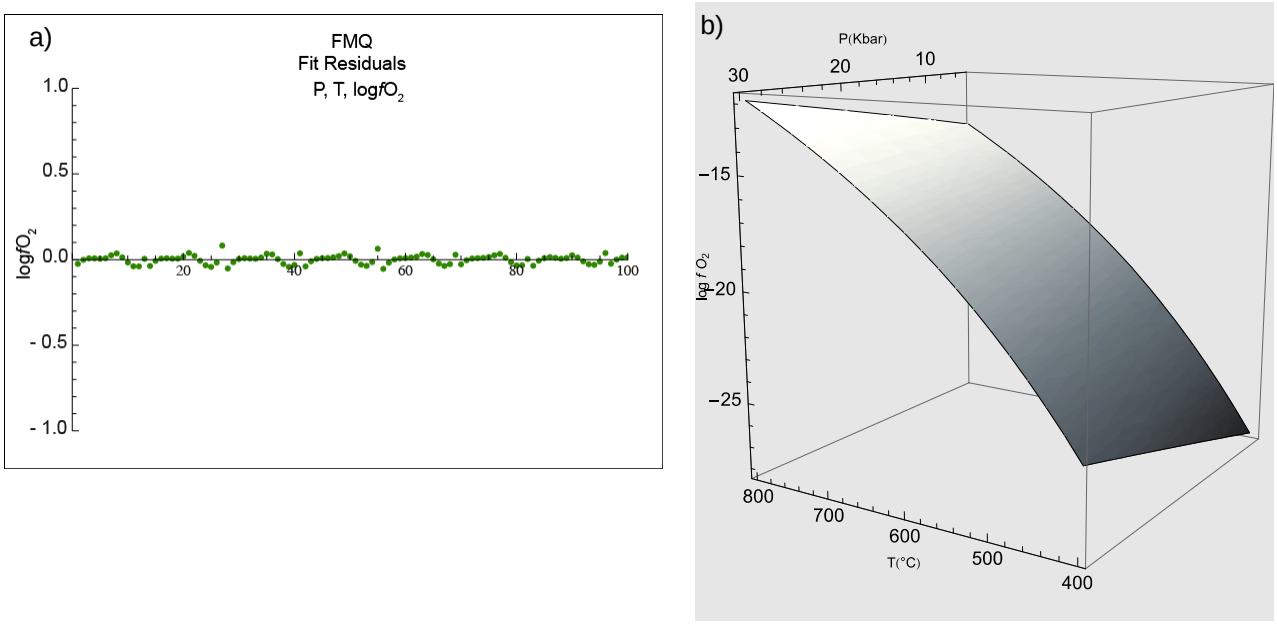

Figure S-4 Residuals from the fit of the FMQ data **(a)** and representation of the fO_2 surface in the P, T, logfO_2 space **(b)**.

Supplementary Information References

Ballhaus, C., Berry, R.F., Green, D.H. (1991) High pressure experimental calibration of the olivine-orthopyroxene-spinel oxygen geobarometer: implications for the oxidation state of the upper mantle. *Contributions to Mineralogy and Petrology* 107, 27-40.

Connolly, J.A. (2005) Computation of phase equilibria by linear programming: a tool for geodynamic modeling and its application to subduction zone decarbonation. *Earth and Planetary Science Letters* 236, 524-541.

Ohmoto, H., Kerrick, D.M. (1977) Devolatilization equilibria in graphitic systems. *American Journal of Science* 277, 1013-1044.

Tumiati, S., Tiraboschi, C., Miozzi, F., Vitale-Brovarone, A., Manning, C.E., Sverjensky, D.A., Milani, S., Poli, S. (2020) Dissolution susceptibility of glass-like carbon versus crystalline graphite in high-pressure aqueous fluids and implications for the behavior of organic matter in subduction zones. *Geochimica et Cosmochimica Acta* 273, 383-402.

Zhang, C., Duan, Z. (2009) A model for C–O–H fluid in the Earth's mantle. *Geochimica et Cosmochimica Acta* 73, 2089-2102.